

FORESHORE EROSION OF KASHIMA COAST BY 2006 AUTUMN STORMS

Elsayed M. GALAL¹, Satoshi TAKEWAKA² and Shinya SASAKURA³

¹ Graduate Student, Dept. of Eng. Mechanics and Energy, University of Tsukuba
(Tsukuba, Ibaraki, 305-8573, Japan)

E-mail:sayed@surface.kz.tsukuba.ac.jp

² Member of JSCE, Associate Professor, Dept. of Eng. Mechanics and Energy, University of Tsukuba
(Tsukuba, Ibaraki, 305-8573, Japan)

E-mail:takewaka@kz.tsukuba.ac.jp

³ Former Graduate student, Dept. of Eng. Mechanics and Energy, University of Tsukuba

Strong low-pressure systems traveled along Japanese Main Island in October 2006. High waves and storm surge attacked Kashima Coast resulting huge erosion over the area. The extent of the study area is 33 km long and bordered by Oarai Port at the north and Kashima Port at the south. This study analyzed the foreshore erosion caused by the impacts of the 2006 storms by estimating the change in the cross sectional area of the subaerial zone using airborne laser data measured in October 2005 and November 2006. The longshore distribution of the cross sectional change indicate that the amount of erosion was less at the sections where headlands are installed compared to sections without them, and the amount of the erosion was decreasing toward the southern part. Total amount of the eroded volume of subaerial zone over the area which reached up to the elevation of T.P. 7 m was 620,000 m³.

A numerical wave ray model was applied to estimate shoaling and refraction effect on the study area in order to investigate wave energy distribution along the shore. Longshore distribution of the wave energy E and longshore component of wave energy flux P_l were averaged over 24 combinations of deep water wave data during the storm hours and compared with the estimated erosion pattern. The results indicate that some of the highly eroded areas in the study area may correspond to the wave energy concentrated areas. The erosion pattern showed a wavy trend, which is similar to the results of E and P_l distributions but with less wave length which may be controlled by the headland locations.

Key Words: *Erosion, Foreshore, Storm, Refraction, Sediment-transport.*

1. INTRODUCTION

Coastal erosion results from beach-ocean interaction coupled with human activity. Combined effect of storm-generated surface waves and storm surges has always posed a severe threat to coastal regions. Quantification of storm-induced beach erosion and subsequent recovery is essential for understanding beach response to abrupt changes in hydrodynamics and appropriately designing coastal engineering projects¹⁾. Previous studies have suggested a number of possible reasons for a longshore-variable storm response^{2),3),4)}.

Nowadays, survey methods using airborne laser measurements have become more common which provides unprecedented detail over large, even regional areas, and has demonstrated great potential for a variety of uses by coastal engineers and

scientists. Many studies about the shoreline definition and subaerial beach change were based on airborne laser measurements^{5),6),7),8)}.

Within this context, the main aim of this paper is to analyze the foreshore erosion caused by the impacts of the 2006 autumn storms on northern part of Kashima Coast and compare the results with the estimated wave energy concentrations along the coast computed by a series of refraction diagrams during the storm event hours.

2. STUDY AREA, METEOROLOGICAL, AND SEA STATE CONDITIONS

The focus of this research is to assess the impacts of the 2006 autumn storms on northern part of Kashima Coast, Ibaraki, Japan, which faces the Pacific Ocean.

The extent of the study area is 33 km long and bordered by Oarai Port at the north and Kashima Port at the south as shown in Fig. 1. There are 28 headlands installed along the coast for shore protection, which are jetty-like structures (shown in Fig. 3 later on).

From 5th to 9th, and from 24th to 26th of October 2006, two strong low-pressure systems traveled along Japanese Main Island. High waves and storm surge caused by pressure fall and strong wind (maximum instantaneous wind speed 37.4 m/s was observed in Choshi) attacked Kashima Coast. Fig. 2 shows the variations of significant offshore wave height $H_{1/3}$ measured every 2 hours, and the variations of tide levels measured every hour of September and October 2006. Offshore waves are measured by the Nationwide Ocean Wave Information Network for Ports and Harbors station at Kashima Port, where the mean water depth is

approximately 24 m. Tide level is measured by the Japanese Meteorological Agency at Choshi Fishery Port.

3. DATA PROCESSING AND EROSION ANALYSES

(1) Airborne laser data

We used and analyzed airborne laser data which have been measured on October 23, 2005 and November 8, 2006. Digital elevation models have been processed above the mean sea water level. Elevation data of the foreshore, backshore, and coastal dune have been assembled with intervals of 10 m in longshore direction and 1m in cross-shore direction along the coordinate system shown in Fig. 3.

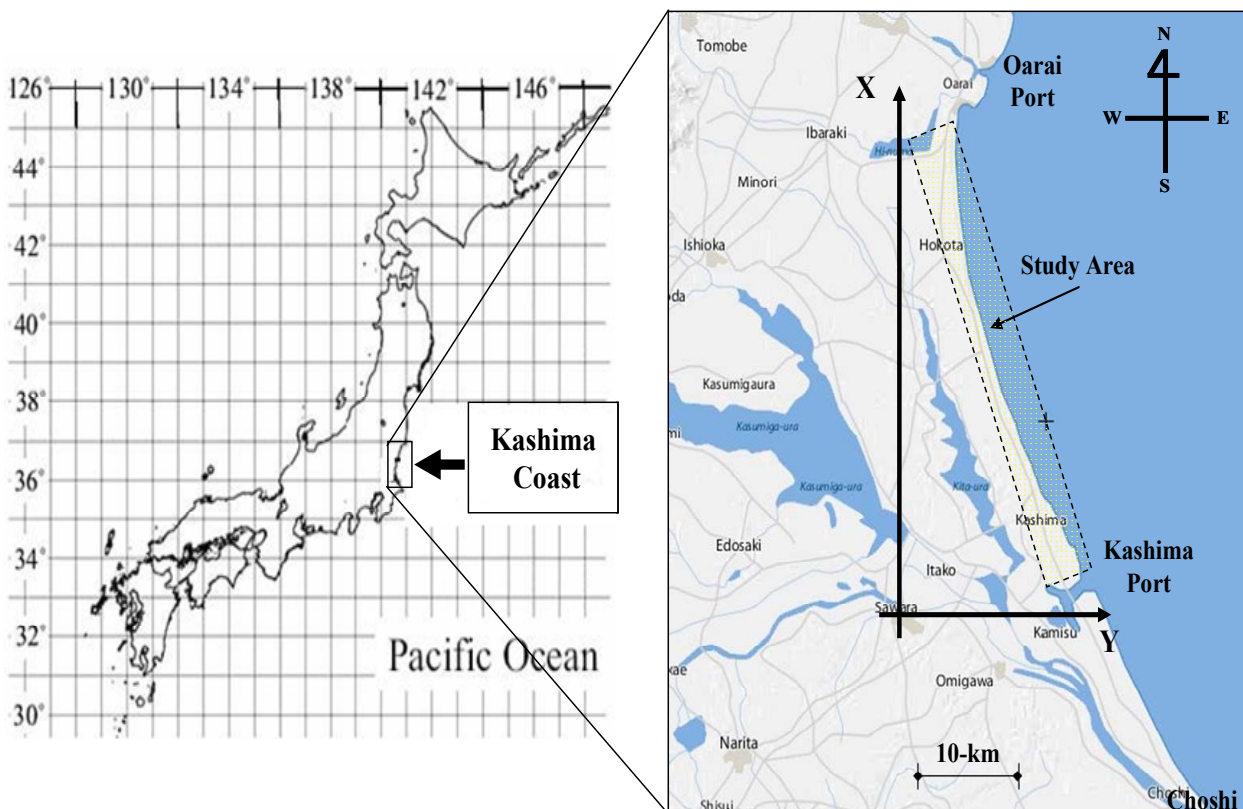


Fig. 1 Research Study Area (Kashima Coast)

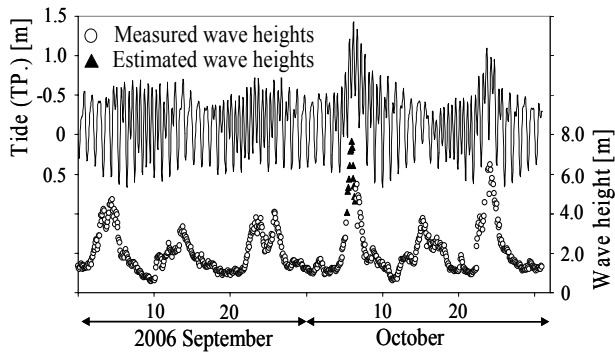


Fig. 2 Time histories of tide level, and wave height $H_{1/3}$. Tide level measured at Choshi Fishery Port, and wave data measured at Kashima Port. Circles indicate measured wave heights while triangles indicate estimated wave heights.

(2) Subaerial beach profiles

The subaerial zone is considered one of the most dynamic places within the active coastal zone where tens of meters of shoreline recession can occur in just a few hours as a result of a major storm. Since the configuration of the coast is slightly concave, we set a longshore reference curve as a baseline for the subsequent analyses. A cubic polynomial was fitted to the coast line and normal transects to the baseline were set as shown in Fig. 3. The interval of the transects is 10 m. Fig. 4 shows typical profiles along the transect located at $X = 15,400$ m estimated from the elevation data of 2005 and 2006, which indicates a considerable variation of cross section within the subaerial zone.

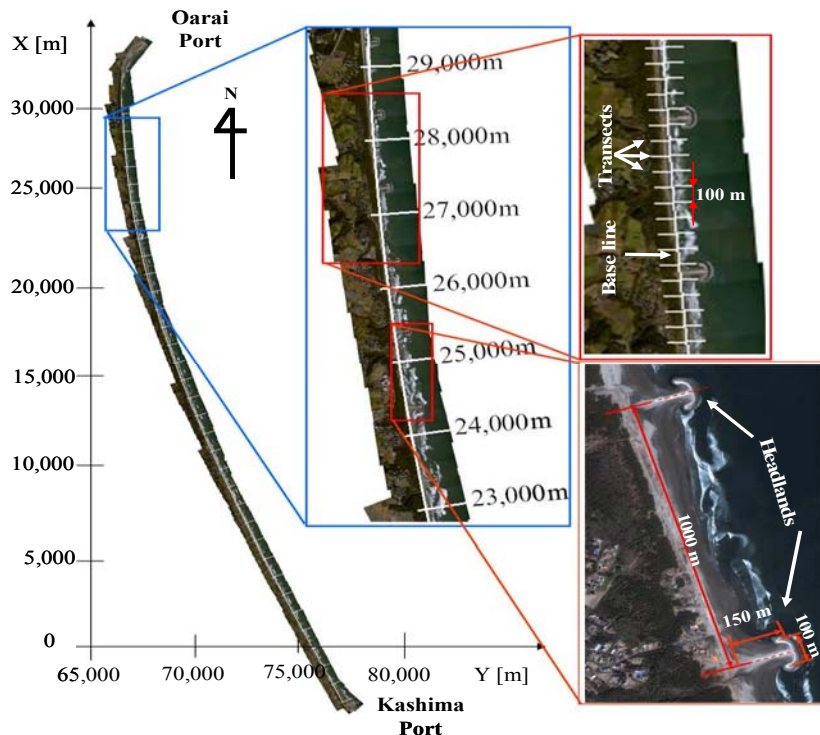


Fig. 3 Aerial photograph of northern part of Kashima Coast with showing the coordinate system and details of headlands.

(3) Longshore distribution of cross sectional change

Fig. 5 shows the longshore distribution of the changes of cross-sectional area. Negative values indicate that subaerial zone was eroded and the squares indicate the locations of headlands. Generally, the result indicates that the amount of erosion is less at the sections where the headlands are installed compared to sections without them. Furthermore, at the locations of the headlands, we observe sudden changes in eroded area. Accumulations are observed in the northern side of the structure whilst the beaches of the southern side have been eroded.

The results displayed in Fig. 5 can be divided into 5 zones according to the pattern of erosion. Zone 1, the variation of the cross sectional change is small and uniform, since the shore is very thin and protected with sea walls and headlands. Zone 2, erosion increased between headlands which may be raised due to the concentration of the wave energy in these areas. Zone 3 has no headland structures, erosion pattern observed here should be close to natural response of an undisturbed beach. Even though there are headlands in zone 4 and zone 5, the overall trend of the variations of the cross sectional changes shows that the amount of the erosion is decreasing toward the southern part which may be raised due to the activation of the longshore sediment transport along this area.

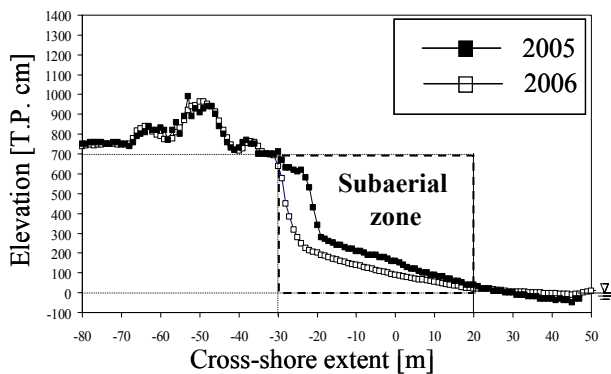


Fig. 4 Typical profile change along a transect X=15,400 m. Tide level (2005) = 0.3 m. Tide level (2006) = 0.0 m

(4) Total amount of eroded volume

Total amount of the eroded volume of subaerial zone after the passage of the low-pressure systems are estimated from the variations of cross shore profiles along each transect of October 2005 and November 2006. The amount of eroded volume along the coast have been estimated by summing up the cross sectional change in the region from T.P. 0.5 m to variable upper limit. Fig. 6 shows the result with the limit of summation as horizontal axis. The figure indicates that erosion in the subaerial zone reached up to the elevation of T.P. 7 m and the total amount of eroded volume over the area was 620,000 m³.

4. NUMERICAL ESTIMATION OF THE WAVE ENERGY CAUSED BY THE STORM

For waves propagating over uneven two-dimensional bathymetry, refraction can cause either a divergence or convergence of wave energy

and associated changes in wave height. In this section, we try to investigate wave energy distribution along the shore on foreshore erosion pattern. The aim is to compare the wave energy distribution estimated from refraction computation for the storm event hours from 6th to 7th October 2006, and the longshore distribution of erosion patterns presented in the pervious section.

1) Wave Ray Computation

A numerical wave ray model was applied to estimate shoaling and refraction on Kashima coastal area. A series of refraction diagrams was computed by changing offshore wave data. Wave periods, directions, and amplitudes used in the numerical simulations were applied from data measurements NOWPHAS at depth of 24 m during the passage of the storm from 6th to 7th October 2006 which is shown in Fig. 7. Some missed wave heights and wave directions were estimated by linear interpolation from the closest wave station.

The changes of wave number k and wave angle θ were computed with a ray tracing procedure^{9),10),11)} in order to provide the wave energy concentration effects in the shallow water. Bathymetry data are supplied in a rectangular-grid format with size of 50 m in x-direction and 20 m in y-direction. The depth contours at every 5.0 m water depths are shown in Fig. 8.

Numerical computation of wave ray patterns was done for every two hours of the selected two days of October, 2006. Fig. 8 shows an example of computed wave-ray patterns which correspond to 16-hr October 7, 2006.

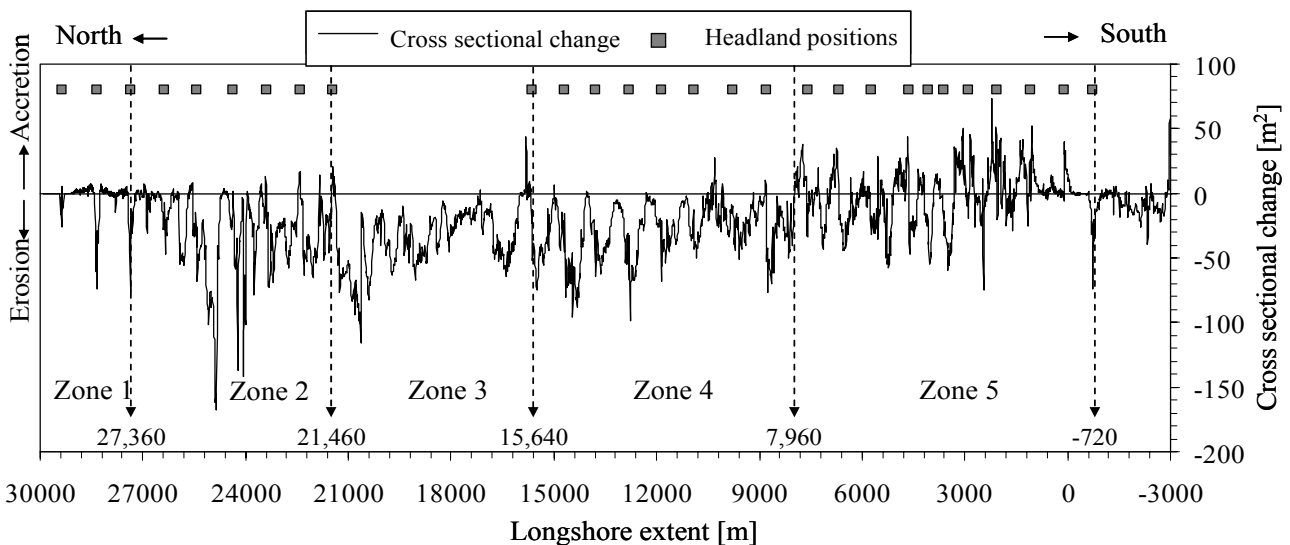


Fig. 5 Longshore distribution of the cross sectional change.

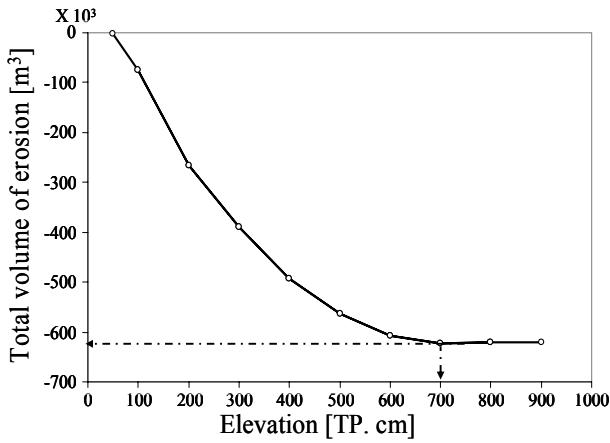


Fig. 6 Total amount of the eroded volume of subaerial zone estimated from the variations of cross shore profiles along each transect of October 2005 and November 2006.

Plotting these ray trajectories can give a good visual indication of the wave transformation due to refraction. Along Kashima Coast, there are regions where rays are converging which indicate wave amplification, whereas divergence of rays indicates reduced wave height.

To determine the wave energy concentration in shallow waters, the number of wave rays reaching in a unit area has been counted for each specific initial deep water condition (H_o , T_o , and θ_o)¹²⁾. Thus, for each chosen combination (H_o , T_o , and θ_o), the energy flux per unit area, in case of the absence of dissipation of energy, reduces to

$$E_o Cg_o b_o = E_s Cg_s b_s \quad (1a)$$

in which E is the energy per unit area, C_g is the group velocity, and b is the local wave ray density.

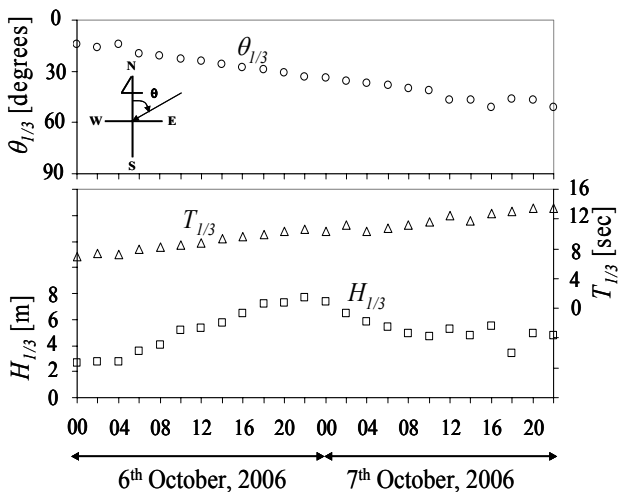


Fig. 7 Storm day 6th and 7th October, 2006 wave data ($H_{1/3}$, $T_{1/3}$, and $\theta_{1/3}$).

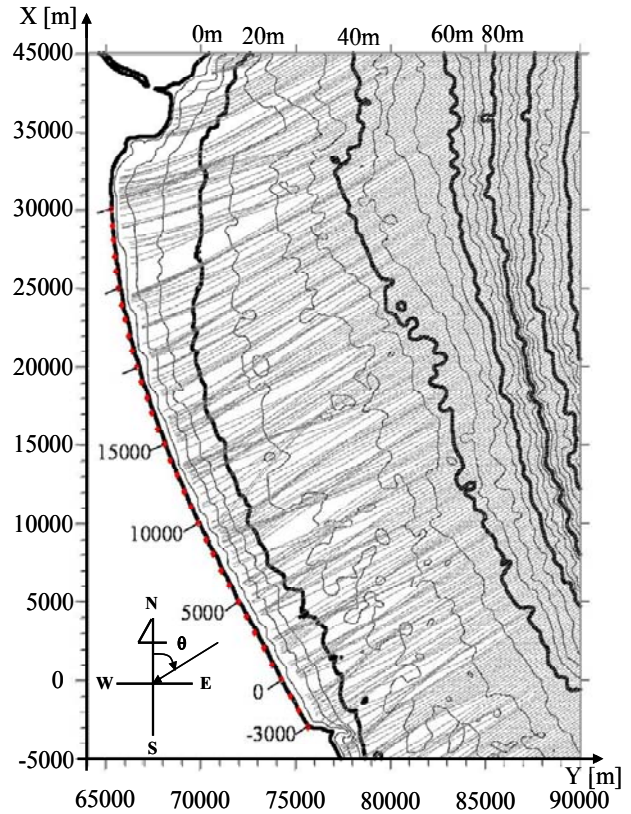


Fig. 8 Wave ray patterns (16hr October 7, 2006) and bathymetric contours. Offshore wave incident angle = 52° and wave period = 10.76 sec.

The subscript letter (o) indicates the offshore areas and (s) indicates nearshore areas and energy per wave length can be determined as

$$E = \frac{1}{8} \rho g H^2 \quad (1b)$$

in which ρ is the mass density ($=1000 \text{ kg/m}^3$), g is the acceleration of gravity, and H is the wave height. Furthermore, an average wave ray angle α with respect to the shore-normal within the unit area, is determined and the longshore component of energy flux P_{ls} , which is a proxy of the driving force for longshore sand transport, is estimated¹¹⁾

$$P_{ls} = E_s Cg_s \sin \alpha \cos \alpha \quad (1c)$$

Longshore distribution of the wave energy E_s and longshore component of energy flux P_{ls} are averaged over 24 combination of (H_o , T_o , and θ_o) during the storm event, and result is presented in Fig. 9. Fig. 10 shows comparisons between E , P_{ls} , and amount of erosion for the 5 zones.

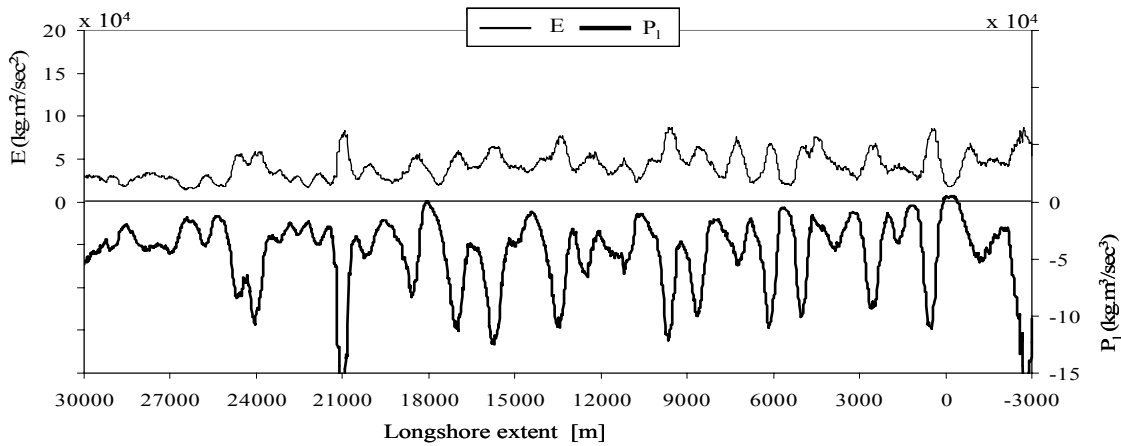


Fig. 9 Longshore distribution of wave energy E and longshore component of wave energy flux P_l .

In shadow box of Fig. 10 (a), which expresses the comparison in Zone 1 and 2, we observe high erosion compared to the other sections and this may be raised due to the sudden increase in E and P_l . In Zone 1, the

wave energy is observed to be small and uniform and this may be considered one of the reasons of the beach stability of this area.

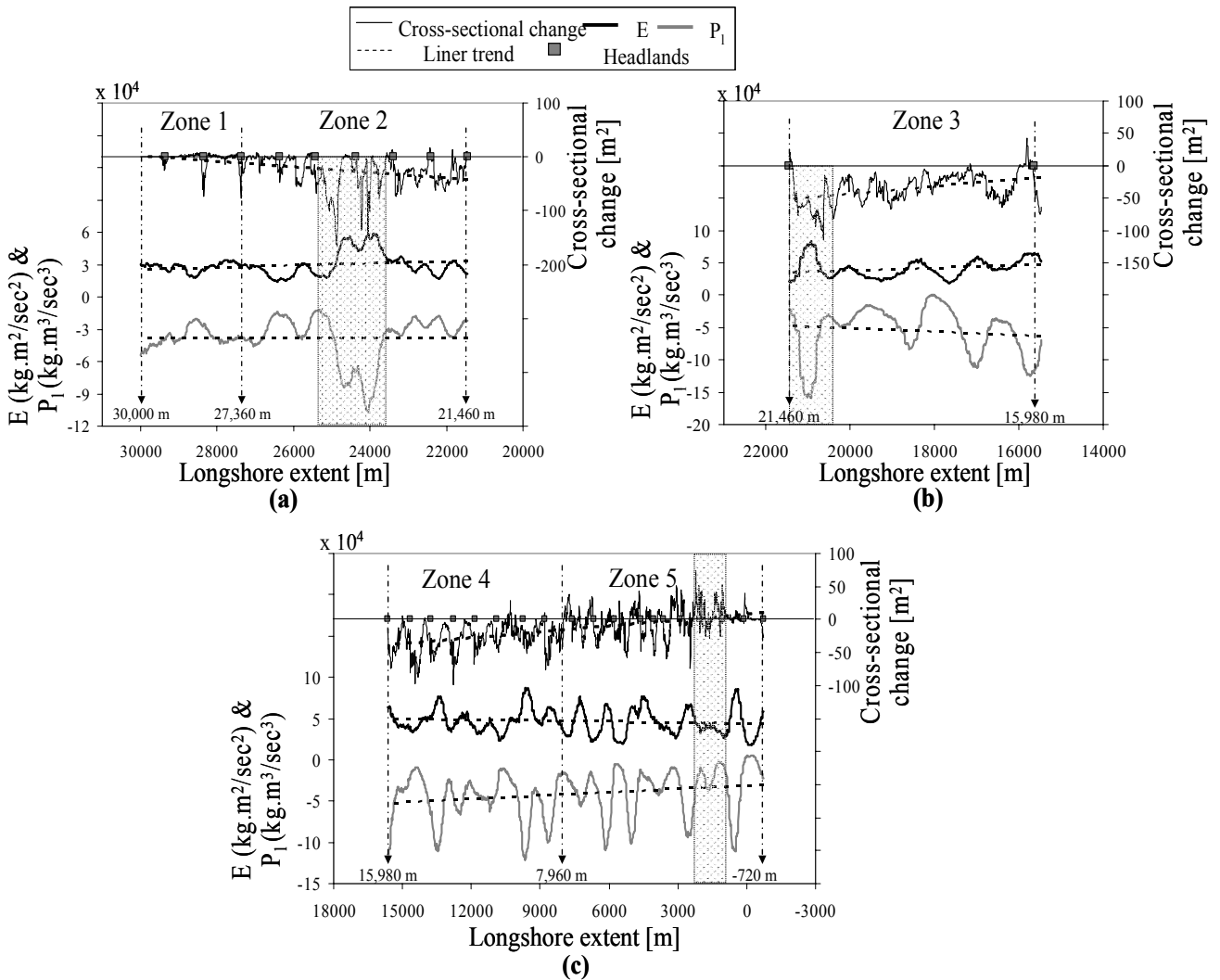


Fig. 10 Comparison between longshore distribution of erosion pattern, E , and P_l . (a) Zone 1 & 2. (b), Zone 3. (c) Zone 4 & 5.

Fig. 10 (b) shows the comparison for Zone 3 where no headlands are installed, and the results indicate that the amount of erosion is decreasing toward the southern part which seems to be a result of the decrease in E and P_l in the same direction. Also, high erosion is observed through in the shadow box which may correspond to the concentration of the wave energy in this area.

Fig. 10 (c) which shows the comparison for Zones 4 and 5 indicating that the amount of the erosion and the energy are decreasing toward the southern part. A considerable amount of accumulation is observed through the shadow box through Zone 5 which may be raised due to the decrease in E and P_l . Generally, the erosion pattern showed a wavy trend which is in accordance with the results of E and P_l , however they may be results of headland effects.

5. CONCLUSIONS

Strong low-pressure systems traveled along Japanese Main Island in October 2006. High waves and storm surge attacked the northern part of Kashima Coast resulting huge erosion over the area. We used and analyzed airborne laser data which have been measured on October 23, 2005 and November 8, 2006. Longshore reference curve and normal transects has been set for the analyses. The foreshore erosion caused by the impacts of the 2006 storms are analyzed by estimating the change in the cross sectional area of the subaerial zone.

The longshore distribution of the cross sectional change indicate that the amount of erosion was less at the sections where headlands are installed compared to sections without them, and the amount of the erosion was decreasing toward the southern part. Total amount of the eroded volume of subaerial zone over the area which reached up to the elevation of T.P. 7 m was 620,000 m³.

A numerical wave ray model was applied to estimate shoaling and refraction effect on the study area in order to investigate wave energy distribution along the shore. A series of refraction diagrams was computed by changing offshore wave data during the passage of the storm from 6th to 7th October 2006. Longshore distribution of the wave energy E and longshore component of wave energy flux P_l were averaged over 24 combinations of deep water wave data during the storm hours and compared with the estimated erosion pattern.

The results indicate that some of the highly eroded areas in the study area may correspond to the wave energy concentrated areas. The erosion pattern showed a wavy trend, which is similar to the results

of E and P_l distributions but with less wave length which may be controlled by the headland locations.

REFERENCES

- 1) Robertson W., Zhang, K., and Whitman, D.: Hurricane-induced beach change derived from airborne laser measurements near Panama City, Florida, *Marine Geology*, vol. 237, pp. 191-205, 2007.
- 2) Ashton, A., List, J.H., Murray, A.B., and Farris, A.S.: Links between erosional hotspots and alongshore sediment transport, *Coast. Sed.* 2003, CD-ROM, 2003.
- 3) Sallenger, A.H.: Storm impact scale for barrier islands. *J. of Coast. Res.* Vol. 16 (3), pp. 890-895, 2000.
- 4) Stockdon H. F., Sallenger, A. H., Holman, R. A., and Howd, P. A.: A simple model for the spatially-variable coastal response to hurricanes, *Marine Geology*, vol. 238, pp. 1-20, 2007.
- 5) Stockdon, H.F., Sallenger, A.H., List, J.H., and Holman, R.A.: Estimation of shoreline position and change using airborne topographic lidar data. *J. of Coast. Res.*, vol. 18 (3), pp. 502-513, 2002.
- 6) Sallenger, A.H., Krabill, W.B., Swift, R.N., Brock, J., List, J., Hansen, M., Holman, R.A., Manizade, S., Sontag, J., Meredith, A., Morgan, K., Yunkel, J.K., Frederick, E.B., and Stockdon, H.F.: Evaluation of airborne topographic lidar for quantifying beach changes. *J. of Coast. Res.*, vol.19 (1), pp.125-133, 2003.
- 7) Sallenger, A.H., Wright, C.W., Guy, K., and Morgan, K.: Assessing storm-induced damage and dune erosion using airborne lidar: Examples from hurricane Isabel, *Shore and Beach*, vol. 72 (2), pp. 3-7, 2004.
- 8) Brock, J.C., Krabill, W.B., and Sallenger, A.H.: Barrier Island Morphodynamic Classification Based on Lidar Metrics for North Assateague Island, Maryland. *J. of Coast. Res.*, vol. 20(2), pp. 498-509, 2004b.
- 9) Dean, R. G. and Dalrymple, R. A.: Water wave mechanics for engineers and scientists, *Advanced Series on Ocean Engineering*, vol. 2, p. 353, 1984.
- 10) Papa, L. and Bertola, R.: A wave refraction computation in the Gulf of Genoa, *Archives for Meteorology, Geophysics, and Bioclimatology Series A*, vol. 32, issue 1-2, pp. 181-189, 1983.
- 11) U.S. Army Coastal Engineering Research Center (CERC): *Shore Protection Manual*, vol 1, New York, 2001.
- 12) Bouws, E. and Battjes, J.A.: A Monte-Carlo approach to the computation of refraction of water waves, *J. Geophys. Res.*, vol. 87, pp. 5718-5722, 1982.